Molecular Cancer

RESEARCH

Open Access

Lactate accumulation induces H4K12la to activate super-enhancer-driven RAD23A expression and promote niraparib resistance in ovarian cancer

Bingfeng Lu[1†], Shuo Chen[1†], Xue Guan[2], Xi Chen[2], Yuping Du[1], Jing Yuan[1], Jielin Wang[1], Qinghua Wu[1], Lingfeng Zhou[1], Xiangchun Huang[1] and Yang Zhao[1,2*]

Abstract

Ovarian cancer is a gynecological malignancy with the highest recurrence and mortality rates. Although niraparib can effectively affect its progression, the challenge of drug resistance remains. Herein, niraparib-resistant ovarian cancer cell lines were constructed to identify the abnormally activated enhancers and associated target genes via RNA in situ conformation sequencing. Notably, the target gene RAD23A was markedly upregulated in niraparib-resistant cells, and inhibiting RAD23A restored their sensitivity. Additionally, abnormal activation of glycolysis in niraparib-resistant cells induced lactate accumulation, which promoted the lactylation of histone H4K12 lysine residues. Correlation analysis showed that key glycolysis enzymes such as pyruvate kinase M and lactate dehydrogenase A were significantly positively correlated with RAD23A expression in ovarian cancer. Additionally, H4K12la activated the super-enhancer (SE) of niraparib and RAD23A expression via MYC transcription factor, thereby enhancing the DNA damage repair ability and promoting the drug resistance of ovarian cancer cells. Overall, the findings of this study indicate that lactic acid accumulation leads to lactylation of histone H4K12la, thereby upregulating SE-mediated abnormal RAD23A expression and promoting niraparib resistance in ovarian cancer cells, suggesting RAD23A as a potential therapeutic target for niraparib-resistant ovarian cancer.

Keywords Niraparib resistance, Super-enhancer, RAD23A, Glycolysis, H4K12la

†Bingfeng Lu and Shuo Chen contributed equally to this work.

*Correspondence:
Yang Zhao
yida.zhaoyang@163.com

Full list of author information is available at the end of the article

Graphical Abstract

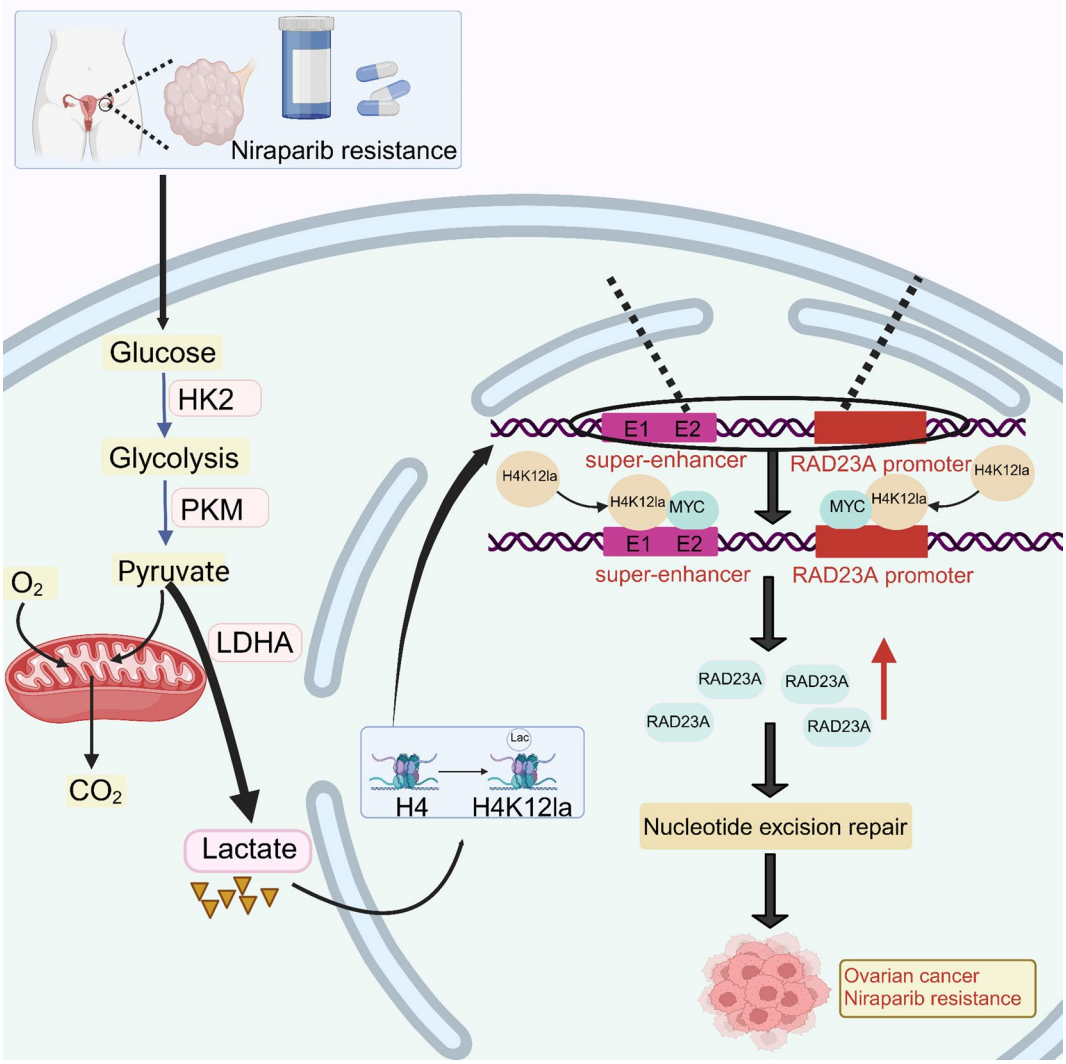

Introduction

Ovarian cancer is one of the three major gynecological malignancies, with a poor prognosis owing to its deep location and challenges of diagnosing and screening early symptoms, and a five-year survival rate of approximately 29.2%, which seriously threatens the lives and health of women worldwide [1–3]. Poly ADP ribose polymerase inhibitors (PARPi) have been widely used in treating ovarian cancer. Many studies have shown the efficacy of PARPi in individuals with BReast Cancer (BRCA) susceptibility gene mutations and those with homologous recombination deficiency (HRD)-positive/BRCA wild-type phenotype; individuals with HRD-negative condition have exhibited lower PARPi efficacy. Nevertheless, the PRIMA study has revealed niraparib as an alternative therapeutic strategy for patients with HRD-negative conditions, as evidenced by a 32% decline in the risk of disease progression or death by niraparib [4]. Based on the results of the PRIMA study, the National Comprehensive Cancer Network guidelines acknowledged the benefits of niraparib in patients with ovarian cancer. However, clinical studies have reported the inevitable development of drug resistance in most patients with ovarian cancer despite initial sensitivity to PARPi, which has become a "bottleneck" for the present ovarian cancer treatment. Therefore, exploring the mechanism of resistance to PARPi and developing strategies to address drug resistance is crucial.

Super-enhancers (SEs) are a group of cis-regulatory elements with strong transcriptional activation properties owing to their transcription factor (TF) recruitment capabilities and promote efficient expression of target genes [5, 6]. Classical SEs form three-dimensional ring structures by binding to target gene promoters, promote

TF recruitment and enhance gene transcription and expression [7, 8]. Reportedly, SEs may be involved in ovarian cancer progression and drug resistance by inducing oncogene expression [9, 10]; however, their mechanism of action in niraparib resistance in ovarian cancer remains unelucidated.

Nucleotide excision repair (NER) is a DNA repair mechanism in organisms for damage in the genome, such as DNA damage caused by ultraviolet rays and antitumor agents such as platinum, making it a drug target for improving the efficacy of cancer treatment [11, 12]. In the NER pathway, the RAD23A gene encodes an important component factor, which forms a complex with xeroderma pigmentosum, complementation group C (XPC; a DNA damage recognition and repair factor) in the nucleus. This complex plays an important role in the early steps of NER, including detecting and repairing DNA damage [13]. These studies suggest that targeting the RAD23A gene may be a potential strategy for reversing cancer drug resistance.

Under aerobic conditions, owing to the "Warburg effect," tumor cells tend to generate notably large amounts of lactic acid compared to normal cells, resulting in increased lactylation of histone and non-histones [14]. Histone lactylation is a novel histone modification discovered in recent years, which participates in cell biological processes by activating the transcription and expression of target genes [15]. However, studies on the biological role of histone lactylation in human ovarian cancer are limited.

This study aimed to investigate the effects of lactate accumulation in niraparib-resistant ovarian cancer cells. Additionally, abnormally activated SEs and associated target genes were identified via RNA in situ conformation sequencing (RIC-seq) to explore the underlying mechanisms of action of niraparib in the cancer cells. To the best of our knowledge, this is the first study reporting that under lactate accumulation, H4K12 lactylation promoted the formation of the SE of niraparib (Nira-SE) upstream of the RAD23A gene and recruited the oncogenic TF MYC to activate the promoter region. This promoted the transcription and expression of the NER factor RAD23A, thereby enhancing the DNA damage repair ability and niraparib resistance in ovarian cancer cells. The results of this study provide insights into the molecular mechanism of niraparib resistance in ovarian cancer and suggest NER-associated RAD23A as a potential therapeutic target for treating niraparib resistance in ovarian cancer.

Methods and materials

Ovarian cancer tissue collection and organoid construction

This study was approved by the Research Ethics Committee of the Third Affiliated Hospital of Guangzhou Medical University (NO: 2024 – 301) and Liaoning Cancer Hospital & Institute [NO: KY20231103], and informed consent was obtained from the patients. Ovarian cancer tissues were obtained from the Department of Gynecology of the Third Affiliated Hospital of Guangzhou Medical University and Liaoning Cancer Hospital & Institute and subjected to histopathology and clinical diagnosis. Ovarian cancer organoids were constructed and analyzed as previously described [16, 17]. Organoids were inoculated in preheated 96-well tissue culture plates in ovarian cancer organoid culture medium: matrix gel (2:3) and cultured in a 5% CO_2 incubator. Treatments (Niraparib and small-interfering RAD23A [siRAD23A]) were initiated concurrently (day 1) and administered once a day for 7 consecutive days. Images were recorded on days 1, 3, and 7 using a microscope (OLYMPUS-CKX53, Japan).

Detection of the size of organoids

Firstly, to avoid bias caused by the individual differences in the response of drugs, we randomly divided the PDOs from the same patients into experimental and control groups ($n = 8$). Secondly, to avoid differences in initial volume, we chose PDOs with initial diameters range between 50 and 150 μm for follow-up analysis. Further, we calculated the area of the analysed organoid on the first and seventh day after drug treatment, and calculated the difference in their areas to assess organoid growth. Finally, the organoids were grouped and measured by different researchers, blinded to data collection to reduce information bias, and the number of statistical organoids per group was 30.

Xenograft tumor experiments

All animal experiments were approved by the Experimental Animal Ethics Committee of the Guangzhou Medical University (NO: S2024-004). Female nude mice (age = 4–6 weeks) were purchased from the Guangdong Experimental Animal Center (Foshan, Guangdong) and subcutaneously inoculated with 2×10^6 niraparib-resistant A2780 (A2780/Nira) cells/each. Following tumor mass formation, all mice were randomly divided into three groups (Control, Niraparib alone: 50 mg/kg, Niraparib combined with siRNA: 5nmol/each). Drug treatments were initiated (day 0) and administered every 3 days thereafter. The tumor sizes were recorded for a total of 21 days. After the experiment, tumor tissues were collected for subsequent immunohistochemical analysis. The tumor size and volume were measured as follows: 0.5 × length × width^2.

Cell culture and construction of niraparib-resistant cell lines

Ovarian cancer A2780 and HO8910 cell lines were purchased from Jennio Biotech (Guangzhou) and cultured in complete Dulbecco's modified Eagle medium and Roswell

Park Memorial Institute 1640 complete medium, respectively. The complete media were supplemented with 1% penicillin–streptomycin and 10% fetal bovine serum. The low-dose escalation method was used to induce niraparib resistance in cell lines to generate A2780/Nira and niraparib-resistant HO8910 (HO8910/Nira) cells, with the gradual increase of the drug concentration from 5 μM to > 40 μM. The drug was induced for at least six months, and its inhibitory concentration of 50% (IC50) was determined. Subsequent experiments were performed when the resistance index was > 3.

CRISPR-cas9 technology

For the CRISPR-Cas9 system, we used purified Cas9 protein as well as targeted sgRNA with low cytotoxicity chemically synthesised (Tsingke Biotech, China) and edited the targeted enhancer region by liposomal transfection. 2×10^5 cells were inoculated in 6-well plate, after attaching, 5 pmol Cas9 protein and sgRNA were added to tube A, supplemented with Opti-MEM to a total volume of 50 μL, and incubated for 10 min at room temperature; 3 μL Lipofectamine 3000 (Thermo, USA) was added to tube B, supplemented with Opti-MEM to a total volume of 50 μL, and incubated for 10 min at room temperature. The solutions in tubes A and B were gently mixed and incubated at room temperature for 20 min, then added to the cells and incubated at 37 °C. The sequence of sgRNA could be found in Supplementary materials Table S2.

Cell counting Kit-8 (CCK-8) assay

Herein, 8×10^3 cells/well were inoculated in a 96-well plate. After complete attachment of the cells, drugs were added, and appropriate drug concentration gradients were set. The cell activity was measured after 48 h using a CCK-8 kit (Yeasen, Shanghai), and the corresponding IC50 values were calculated.

5-Ethynyl-2′-deoxyuridine (EdU) assay

For the EdU assay, 6×10^3 cells/well were inoculated into a 96-well plate. After complete attachment of the cells, drugs were added, and the plate was cultured in a CO_2 incubator for 48 h. The culture media were replaced with fresh complete media containing EDU (1:200) and further incubated for 2 h. The EdU assay was performed per the instructions of the reagent manufacturer, and the plates were observed and photographed using a fluorescence microscope. The Image J software was used to count the proportion of EdU-positive cells.

Colony formation assay

Herein, 500–1000 cells were inoculated into each well of a six-well plate. After complete attachment of the cells, the drugs were added. Following 7–10 days of incubation, a cloned cell group of > 50 cells was observed in the control group. The culture media were discarded, and the cells were washed with phosphate-buffered saline (PBS), fixed with 4% paraformaldehyde at 20–25℃ for 15 min, washed with PBS, stained with 0.1% crystal violet for 15 min, washed with PBS and fully dried, and then photographed. The Image J software was used to count the number of cell clones in each group.

Immunofluorescence experiments

For the immunofluorescence assay, 2×10^4 cells/well were inoculated into a 24-well plate containing a cell slide. Drugs were added after complete attachment of the cells, and the cells were cultured for 48 hours. The cells were fixed with 4% paraformaldehyde for 15 minutes at room temperature, followed by two rounds of washing with PBS. They were then penetrated with Triton X-100 (Beyotime, Shanghai) for 15 minutes and washed twice with PBS. Subsequently, the cells were blocked with 5% bovine serum albumin (BSA) for 1 hour. The γ-H2AX antibody (1:200, Abclonal, Wuhan) was added, and the samples were incubated overnight at 4°C. Upon the completion of incubation, the cells were washed thrice with 1× PBS-Tween 20 (PBST) for 5 minutes/wash. The fluorescent secondary antibody (1:500, Proteintech, Wuhan) was then applied, and the cells were subject to wash thrice with 1 × PBST for 5 minutes/wash. Finally, the 4′,6-diamidino-2-phenylindole staining solution containing antifade was added, sealed, and photographed using a confocal microscope.

Comet experiment

Drug-treated cells were digested with trypsin, resuspended by centrifugation, and prepared into a 1×10^6 cell suspension in PBS. The comet assay was performed per the instructions of the reagent manufacturer (Comet Assay Kit, Beyotime). After completing the single-cell gel electrophoresis, the cells were neutralized, stained, washed, and observed under a fluorescence microscope and photographed.

Quantitative polymerase chain reaction (qPCR) assay

The total RNA was extracted using the RNA extraction reagent RNAiso Plus (TaKaRa) and was reverse transcribed to obtain the complementary DNA using a reverse transcription kit (Yeasen). A qPCR reaction system (Hieff® qPCR SYBR Green Master Mix, Yeasen) was prepared, and the target gene was amplified using a qPCR instrument to obtain the corresponding CT value (QuantStudio 3, USA). The relative gene expression was calculated using the $2^{-\Delta\Delta CT}$ method.

Western blotting

The protein samples were isolated using the Intact-Protein™ lysis kit (GenuIN, Hefei) containing 1 mM

phenylmethylsulfonyl fluoride (PMSF) for lysis on ice for 15 min. The bicinchoninic acid protein quantification kit (Beyotime) was used for protein quantification, and the proteins were denatured at 95 °C for 10 min in a loading buffer system containing mercaptoethanol. Different concentrations of polyacrylamide gel were selected for electrophoresis according to the molecular weight of the target protein. After the electrophoresis, proteins were transferred to polyvinylidene fluoride membranes, which were then blocked with 3% BSA at room temperature for 90 min. Next, the membrane was added with primary antibodies for the target protein and incubated at room temperature for 2 h. After washing thrice with 1×TBST for 10 min/wash, the membrane was incubated with a secondary antibody at room temperature for 1 h, again washed thrice with 1× TBST for 10 min/wash, and then photographed using NaQ™ ECL Substrate Kit (GenuIN).

Co-immunoprecipitation (CO-IP) experiment

Protein samples were collected and added with the immunoprecipitation lysis buffer (Beyotime) containing 1 mM PMSF. The protein was quantified to 5 μg/μL. Next, 500 μL of protein lysis buffer was taken from each group, and the CO-IP assay (Co-Immunoprecipitation Kit, BersinBio) was performed per the instructions of the reagent manufacturer. The proteins were detected by western blotting.

Chromatin immunoprecipitation (ChIP) assay

After the cells reached > 90% confluence, the culture media was replaced with fresh complete culture media containing 1% formaldehyde and incubated at 37 °C for 10 min. After cross-linking and fixation of the intracellular proteins and DNA complexes, the ChIP assay was performed per the instructions of the manufacturer (BeyoChIP™ Enzymatic ChIP, Beyotime). Finally, the isolated DNA was subjected to qPCR.

Lactic acid content detection

Digest the cells in a 10 cm culture dish and take 2*107 cells for detection. Perform the experiment according to the instructions of the reagent manufacturer (Lactic acid content (LA) detection kit, Solarbio), use an Enzyme-labeled instrument to detect the absorbance value at 570 nm, and calculate the corresponding lactic acid concentration.

RIC-seq and SE identification

The promoter–enhancer interaction signals in the niraparib-resistant cells were detected by RIC-seq. The sequencing and result analysis were performed by Guangzhou Epibiotek Co., Ltd (Guangzhou, China), and the specific experimental steps described by Xue et al. were referred to for RIC-seq [18].

Bioinformatics analysis

The GEPIA2 (http://gepia2.cancer-pku.cn/) and Sparkle (https://grswsci.top/) online platform were used to an alyze the differential gene expression or correlation in ovarian cancer. The GSE datasets were downloaded from the Gene Expression Omnibus database (http://www.ncbi.nlm.nih.gov/geo), namely GSE40595 and GSE66957, and were used to analyze the expression of related genes using R. The KMplot (https://kmplot.com/) and GEPIA2 online platform were used to analyze the prognosis of patients with ovarian cancer. The FANTOM5 platform (https://fantom.gsc.riken.jp/5/) was used to screen and visualize gene enhancer regions on the IGV software. The TFs of the RAD23A gene were predicted using four TF prediction websites, based on JASPAR/PROMO/Cistrome/ENCODE.

Data analyses

Data were analyzed using the GraphPad Prism 8.0 software, and cell number and grayscale value analyses were performed using the ImageJ software. All experiments were repeated at least thrice. The student's T-test was used to compare the data between the two groups. One- or two-way analysis of variance was used to compare the data between multiple groups with 95% confidence intervals. The P-value of < 0.05 denoted statistical significance.

Results

RIC-seq-derived interaction map between SEs and target gene promoters in niraparib-resistant ovarian cancer cells

To obtain the interaction map between SEs and their target genes associated with niraparib resistance in ovarian cancer, A2780/Nira and HO8910/Nira cells were generated using carboplatin (10 μM) for 48 h to simulate drug-induced DNA damage, and then using the drug concentration gradient method to induce niraparib resistance (Fig. 1A). The CCK-8 assay revealed the IC50 value of niraparib (Fig. 1B–E). RIC-seq data of A2780/Nira and HO8910/Nira cells was combined with the public enhancer data to obtain the interaction map between SEs and their target genes regarding niraparib resistance (Fig. 1F, Supplementary materials Table S6). RIC-seq sequencing detected the frequent interaction of the SE region at chr19:13004808–13,072,187 (named Nira-SE) with promotors of target genes, including RAD23A, RNU2-2P, WDR74, and RP11-424C20.2. Among them, Nira-SE interacted most significantly with the RAD23A promoter region (Fig. 1G).

In vitro, in vivo, and organoid experiments show that targeting RAD23A reversed niraparib resistance in ovarian cancer

To clarify the role of RAD23A in niraparib resistance in ovarian cancer, RAD23A expression in ovarian cancer

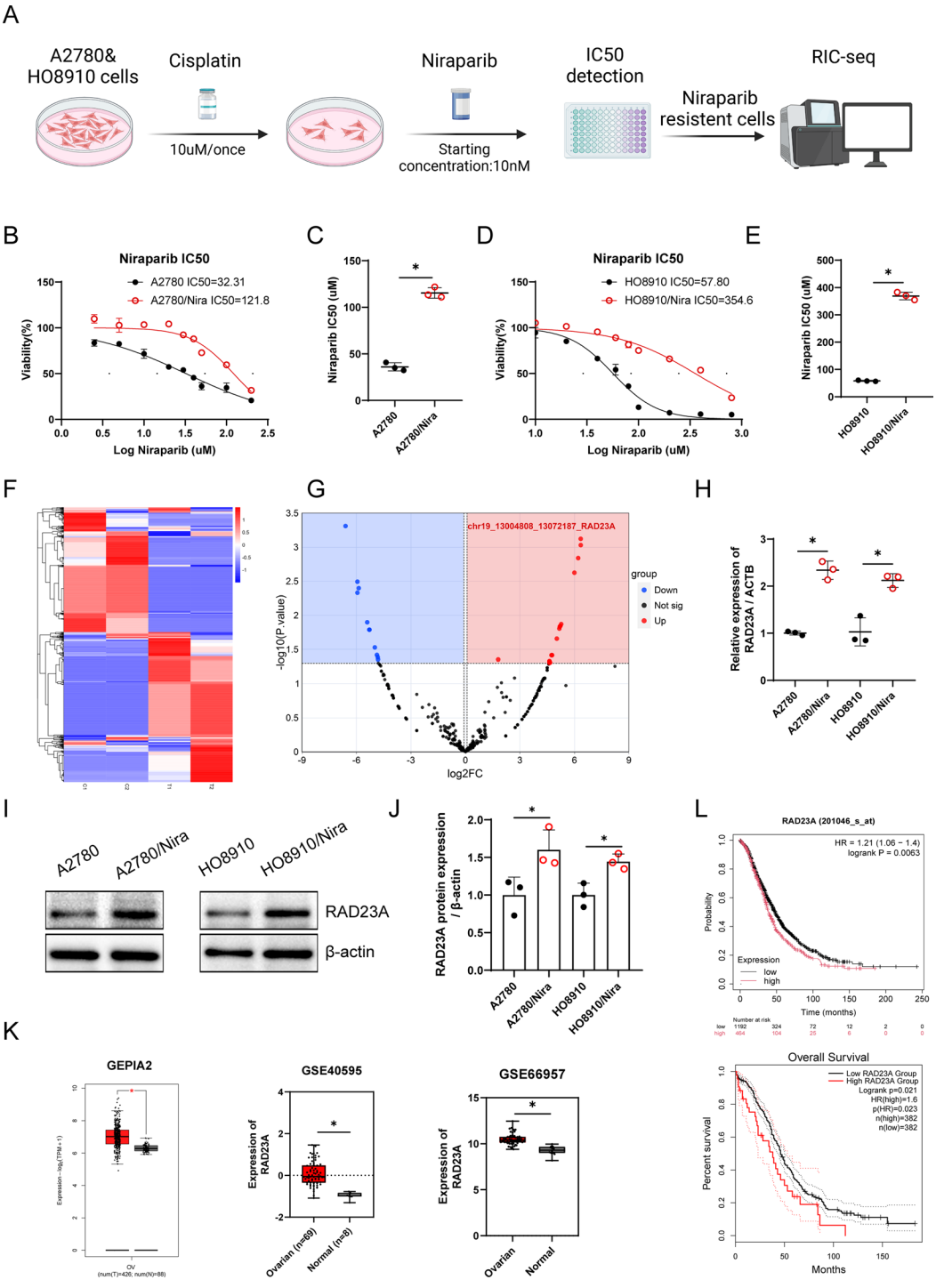

Fig. 1 RIC-seq characterizes the interaction map between super enhancers and target gene promoters in niraparib resistance in ovarian cancer. (**A**). Consructions of Niraparib resistant cells and RIC-seq. (**B**-**C**) IC50 detection of Niraparib in A2780 and A2780/Nira cells. (**D**-**E**) IC50 detection of Niraparib in HO8910 and HO8910/Nira cells. (**F**) RIC-seq sequencing shows a heat map of the interaction between aberrantly activated super enhancers and target genes in A2780/Nira cells. (**G**) Volcano plot showing that the super enhancer Nira-SE interacts most frequently with the target gene RAD23A. (**H**) QPCR detection of RAD23A mRNA levels in Niraparib-resistant and parental cells of ovarian cancer. (**I**-**J**) Detection of RAD23A protein levels in Niraparib-resistant and parental cells of ovarian cancer. (**K**) Expression levels of RAD23A in GEPIA2, GSE40595, and GSE66957 ovarian cancer datasets. (**L**) KMplot-OV database analysis of the relationship between RAD23A and overall survival of ovarian cancer patients. *$p < 0.05$

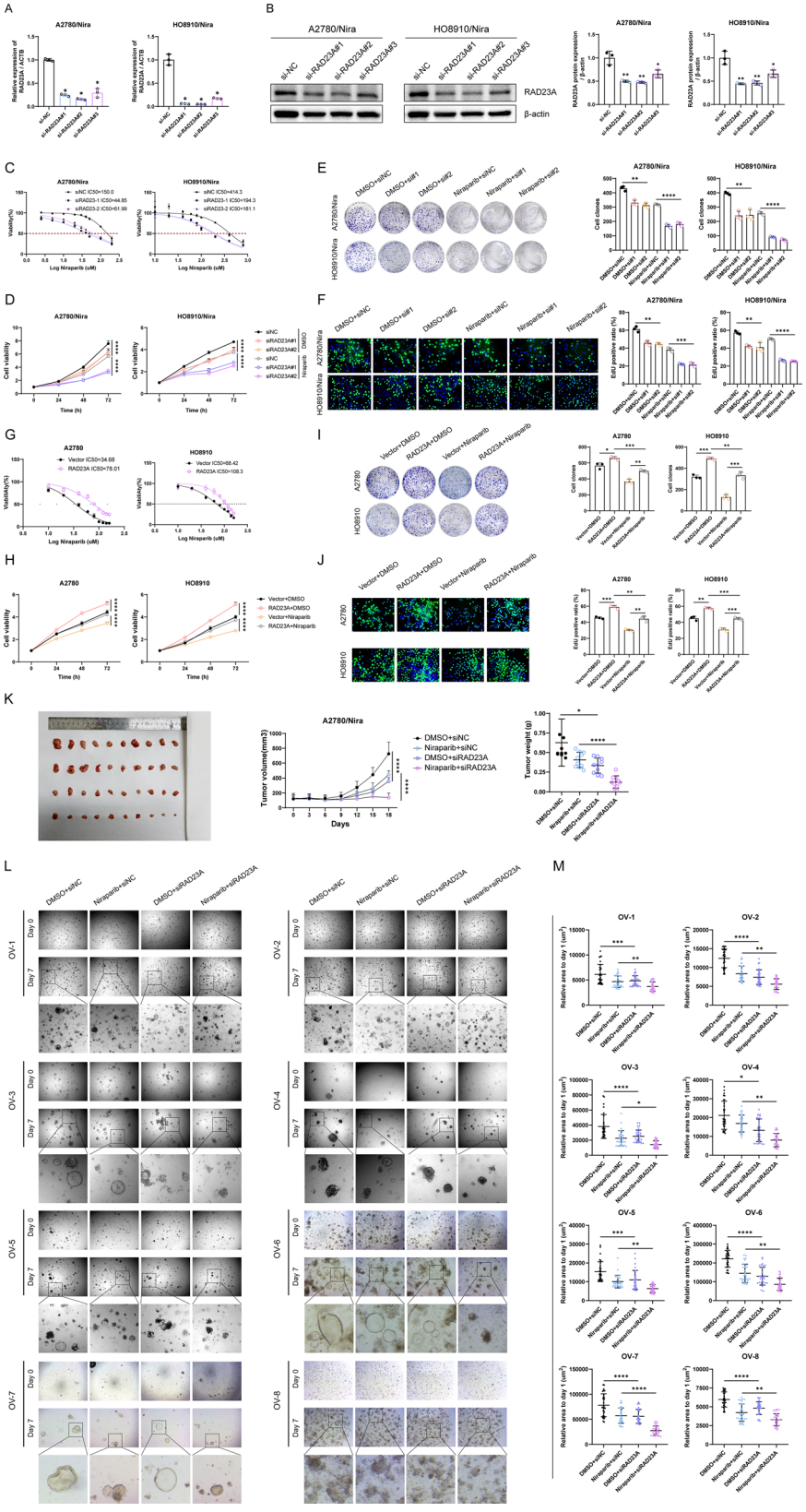

Fig. 2 (See legend on next page.)

(See figure on previous page.)

Fig. 2 In vitro and vivo as well as organoid experiments showed that targeting RAD23A reversed niraparib resistance in ovarian cancer. (**A**-**B**) RNA and protein levels of knockdown RAD23A in A2780/Nira and HO8910/Nira cells. (**C**) Detection of the IC50 of Niraparib after knockdown of RAD23A in Niraparib-resistant cells. (**D**) Detection of cell viability after knockdown of RAD23A in Niraparib-resistant cells. (**E**) Detection of clone formation ability after knockdown of RAD23A in Niraparib-resistant cells. (**F**) EdU assay to detect cell proliferation ability after knockdown of RAD23A in Niraparib-resistant cells. (**G**-**J**) RAD23A overexpression increased Niraparib resistance and cell proliferation ability in platinum-pretreated A2780 and HO8910 cells. (**K**) Xenograft tumor experiment showed that compared with the siNC group, the siRAD23A group exhibited significant inhibition of subcutaneous tumor formation; the combination of siRAD23A and niraparib group exhibited significant inhibition of subcutaneous tumor formation than siNC + niraparib group, the tumor volume in the siRAD23A combined with Niraparib treatment group was the smallest. (**L**-**M**) The ovarian cancer organoid experiment showed that compared with the siNC group, the siRAD23A group exhibited significant inhibition of the growth of organoids; the combination of siRAD23A and niraparib group also exhibited significant inhibition of the growth of organoids than siNC + niraparib group. The bar graph shows the statistical analysis of the 30 organoids in each group. The microscopic imaging ratio is 4 × 10 times. *$p < 0.05$, **$p < 0.01$, ***$p < 0.001$, ****$p < 0.0001$

cell lines A2780, A2780/Nira, HO8910, and HO8910/Nira was analyzed. Notably, the messenger RNA (mRNA) and protein levels of RAD23A in niraparib-resistant cells were higher than those in the non-resistant cells (Fig. 1H-J). The analysis of GSE40595, GSE66957 datasets and GEPIA2 website [19, 20] revealed that RAD23A expression was increased in ovarian cancer tissues (Fig. 1K), and the KMplot [21] survival analysis and GEPIA2 datasets associated high expression of RAD23A with poor prognosis in ovarian cancer (Fig. 1L).

To evaluate the function of RAD23A in niraparib-resistant ovarian cancer cells, siRAD23A was transfected to knock down RAD23A expression (Fig. 2A and B). The CCK-8 assay showed RAD23A knock-down increased the sensitivity of ovarian cancer cells to niraparib (Fig. 2C and D). Furthermore, colony formation and EdU assays revealed that the proliferation ability of niraparib-resistant cells markedly reduced after RAD23A knock-down (Fig. 2E and F). Besides, RAD23A overexpression increased Niraparib resistance and cell proliferation ability in platinum-pretreated A2780 and HO8910 cells (Fig. 2G-J).

A xenograft tumor model of niraparib-resistant cells and an organoid model derived from patients with ovarian cancer were constructed to verify the in vivo therapeutic effects of RAD23A. Notably, compared with the siNC group, the siRAD23A group exhibited significant inhibition of subcutaneous tumor formation; the combination of siRAD23A and niraparib group exhibited significant inhibition of subcutaneous tumor formation than siNC + niraparib group (Fig. 2K). Similarly, analysis of organoids revealed that compared with the siNC group, the siRAD23A group exhibited significant inhibition of the growth of organoids; the combination of siRAD23A and niraparib group also exhibited significant inhibition of the growth of organoids than siNC + niraparib group (Fig. 2L and M).

RAD23A is involved in niraparib resistance in ovarian cancer by regulating DNA damage repair

RAD23A, an important component of the NER pathway, repairs DNA damage caused by various factors such as ultraviolet radiation and chemical drugs. Therefore, its ability to repair DNA damage was assessed in niraparib-resistant ovarian cancer cells. Immunofluorescence experiments showed that the overexpression of RAD23A could decrease γ-H2AX expression, a double-strand DNA damage marker, in platinum-pretreated A2780 and HO8910 cells (Fig. 3A-B). Furthermore, the comet assay confirmed reduced degree of DNA damage following RAD23A overexpression, which suggest that high levels of RAD23A could increase DNA damage repair (Fig. 3C-D). Besides, downregulating RAD23A markedly increased DNA damage (Fig. 3E-H). Similarly, immunohistochemistry results of mouse xenograft tumor tissues showed that the siRAD23A + niraparib group exhibited a notable increase in γ-H2AX expression (Fig. 3I). These results suggest that RAD23A is involved in niraparib resistance in ovarian cancer by regulating DNA damage repair.

Nira-SE regulates the expression of the target gene RAD23A

Bioinformatics analysis was performed to clarify the mechanism of epigenetic remodeling of RAD23A in chemotherapy resistance in ovarian cancer. Notably, two enhancers chr19:13023589–13,024,232 and chr19:13048278–13,048,689, named E1 and E2, respectively, were identified in the Nira-SE region on FANTOM5 portal [22] (Fig. 4A). Next, the clustered regularly interspaced short palindromic repeats (CRISPR)-CRISPR-associated protein 9 (Cas9) technology was utilized to knock out E1 and E2 (Fig. 4B and C) to evaluate their effects on the transcriptional activity of RAD23A. The qPCR and western blotting results showed that knocking out either E1 or E2 markedly reduced RAD23A expression, with further downregulation of RAD23A expression after the combined knockout of E1 and E2 (Fig. 4D and E).

Local disruption of Nira-SE reverses chemoresistance in ovarian cancer

The effects of blocking Nira-SE on niraparib resistance in ovarian cancer were assessed. Specifically, E1 and E2 were knocked out in A2780/Nira and HO8910/Nira cells. The CCK-8 assay showed E1 or E2 knock-out increased the

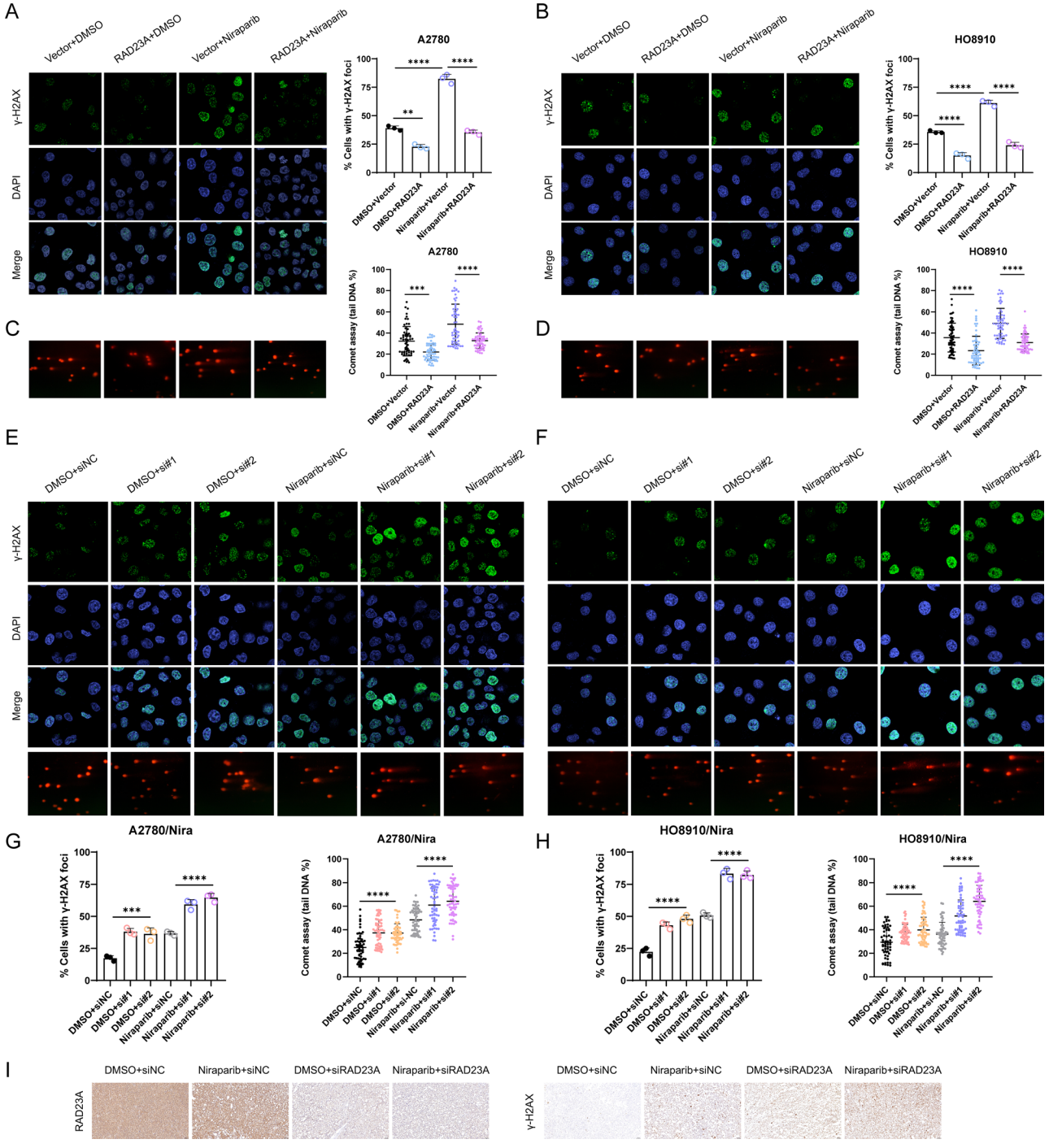

Fig. 3 RAD23A regulates DNA damage repair in Niraparib-resistant ovarian cancer. (**A**-**B**) Immunofluorescence shows decreased level of γ-H2AX after RAD23A overexpression in A2780 and HO8910 cells, Nikon confocal imaging: 60x. (**C**-**D**) Comet assay shows decreased DNA damage levels after RAD23A overexpression in A2780 and HO8910 cells, microscopic imaging ratio: 20 × 10x. (**E**-**H**) the level of γ-H2AX and DNA damage levels after knocking down RAD23A in A2780/Nira and HO8910/Nira cells. (**I**) Immunohistochemistry shows that the γ-H2AX level in the siRAD23A combined with Niraparib treatment group was the highest compared to the control group and Niraparib alone group. $^{**}p < 0.01$, $^{***}p < 0.001$, $^{****}p < 0.0001$

sensitivity of resistant cells to niraparib (Fig. 4F and G). Furthermore, colony formation and EdU assays showed that the proliferation of niraparib-resistant cells considerably decreased after E1 or E2 knock-out (Fig. 4H and I). Moreover, after E1 or E2 knock-out, γ-H2AX expression significantly increased (Fig. 4J; immunofluorescence assay) and the degree of DNA damage was aggravated (Fig. 4K; comet assay).

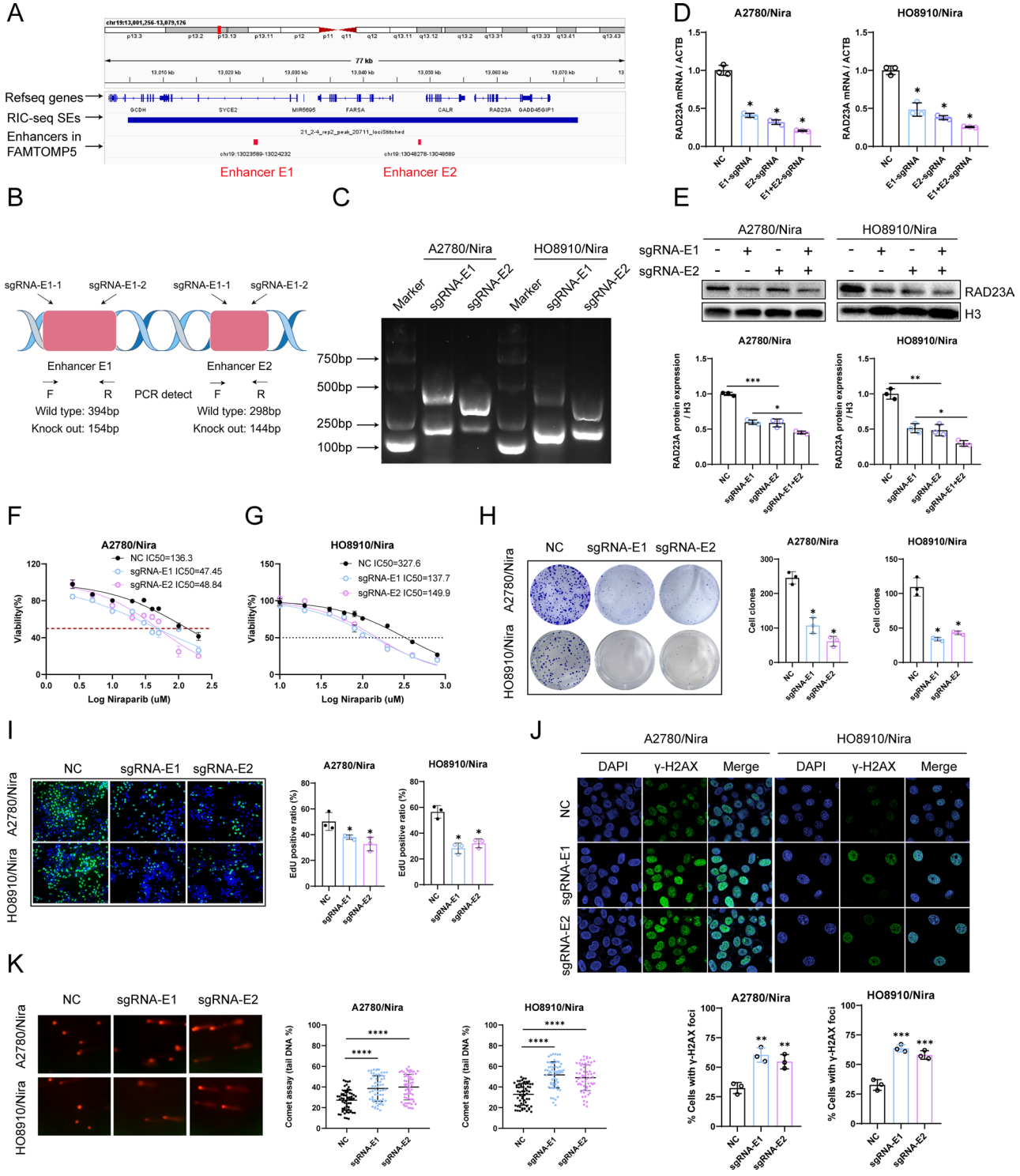

Fig. 4 Blocking super enhancers effectively reduces RAD23A expression and reverses Niraparib resistance in ovarian cancer. (**A**) The enhancers E1 and E2 in the Nira-SE region are shown in the FAMTOMP5 database and visualized using IGV software. (**B**) Specific sgRNAs targeting enhancers E1 and E2 were designed, and E1 and E2 were knocked out using CRISPR-Cas9 technology; (**C**) DNA gel electrophoresis showed partial knockout of E1 and E2 in A2780/Nira and HO8910/Nira cells. (**D**) Detection of RAD23A mRNA level after knockout of enhancers E1 and E2 in Niraparib-resistant cells. (**E**) Detection of RAD23A protein level after knockout of enhancers E1 and E2 in Niraparib-resistant cells. (**F**-**G**) Detection of the IC50 of Niraparib after knockout of enhancers E1 or E2 in Niraparib-resistant cells. (**H**) Detection of clone formation ability after knockout of enhancers E1 or E2 in Niraparib-resistant cells. (**I**) EdU assay to detect cell proliferation ability after knocking out enhancer E1 or E2 in Niraparib-resistant cells. (**J**) Immunofluorescence to detect the level of DNA damage marker γ-H2AX after knocking out enhancer E1 or E2 in Niraparib-resistant cells. (**K**) Comet assay showed that the level of cellular DNA damage increased after knocking out enhancer E1 or E2 in A2780/Nira and HO8910/Nira cells. *$p < 0.05$, **$p < 0.01$, ***$p < 0.001$, ****$p < 0.0001$

Nira-SE promotes the recruitment of the oncogenic TF MYC to the promoter

TFs mediate the SE regulatory network and initiate transcription in a gene-specific manner. Hence, TFs involved with RAD23A were identified utilizing the JASPAR, PROMO, Cistrome, and ENCODE databases by intersecting the prediction results of the four databases. In total, seven TFs were identified, namely yin yang 1 (YY1), upstream transcription factor 2 (USF2), myelocytomatosis (MYC), E2F Transcription Factor 1 (E2F1), v-rel reticuloendotheliosis viral oncogene homolog A (RELA), γ-aminobutyric acid transporter 1(GATA1), and Upstream Transcription Factor 1 (USF1) (Fig. 5A), and their roles in ovarian cancer were verified. Notably, MYC knock-down significantly decreased the mRNA (Fig. 5B and C) and protein (Fig. 5D–F) levels of RAD23A. The ChIP-qPCR analysis showed that MYC was enriched in the RAD23A promoter (Fig. 5G and H),

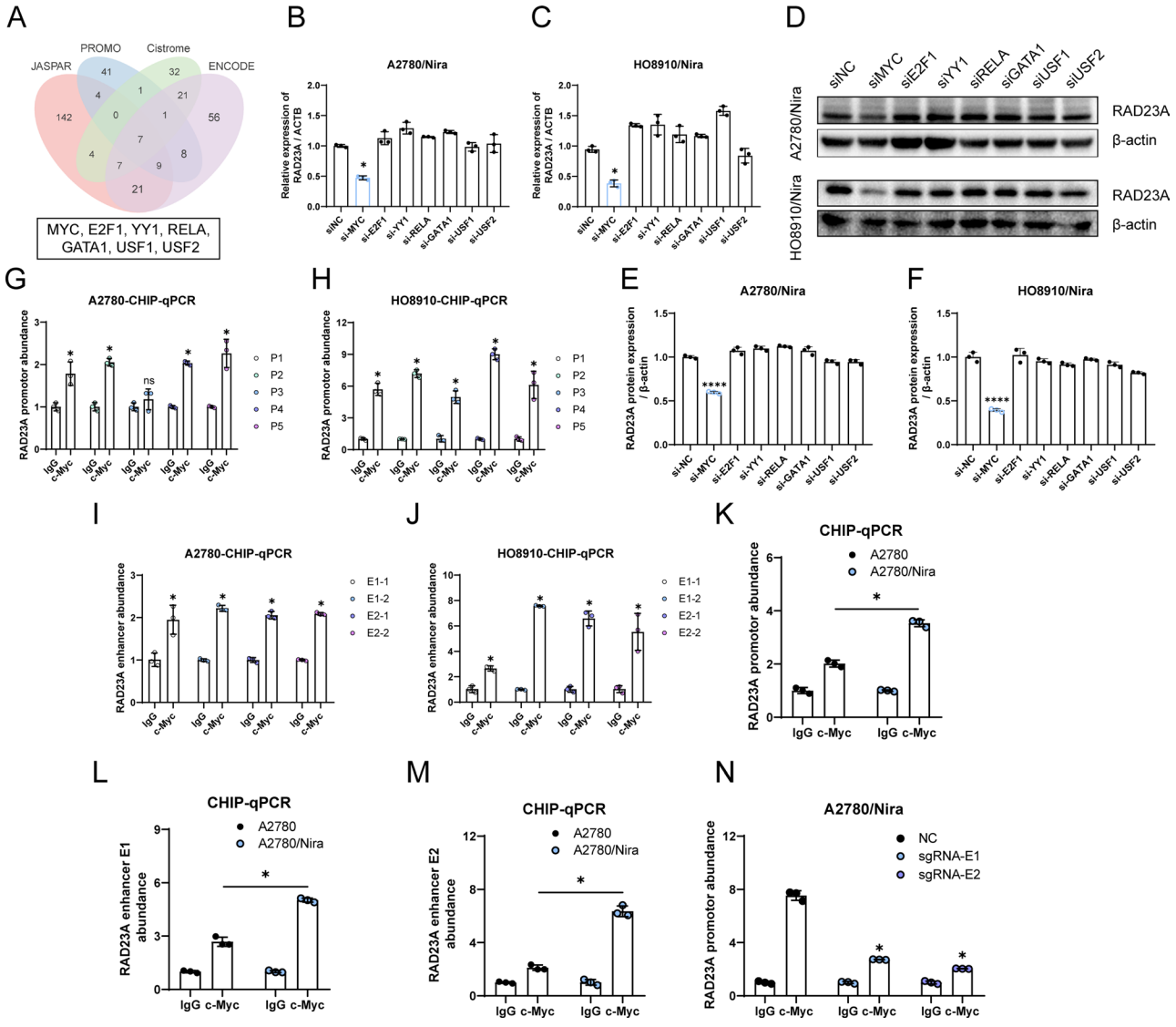

Fig. 5 Super-enhancer Nira-SE promotes the recruitment of the oncogenic transcription factor MYC to the promoter. (**A**) The JASPAR, PROMO, Cistrome and ENCODE databases predict the transcription factors of RAD23A. The intersection shows that YY1, USF2, MYC, E2F1, RELA, GATA1 and USF1 are the possible transcription factors of RAD23A. (**B**-**C**) The above seven transcription factors were knocked down in ovarian cancer resistant cells. The results showed that when the transcription factor MYC was knocked down, the mRNA level of RAD23A was significantly decreased. (**D**-**F**) When the transcription factor MYC was knocked down, the protein level of RAD23A was significantly decreased. (**G**-**H**) CHIP-qPCR detected the enrichment of transcription factor MYC in the promoter region of RAD23A. P1-P5 represent primers in 5 different regions on the RAD23A promoter. (**I**-**J**) CHIP-qPCR detected the enrichment of transcription factor MYC in the E1 and E2 regions of RAD23A enhancer. Two pairs of primers were designed for each region. (**K**) MYC is enriched more on the RAD23A promoter in ovarian cancer resistant cells. (**L**-**M**) MYC is enriched more on enhancers E1 and E2 in ovarian cancer resistant cells. (**N**) Knocking out enhancers E1 and E2 in ovarian cancer resistant cells significantly reduced the enrichment of transcription factor MYC in the RAD23A promoter region. ns means $p > 0.05$, *$p < 0.05$, **$p < 0.01$, ***$p < 0.001$, ****$p < 0.0001$

enhancer E1, and E2 region (Fig. 5I and J) of A2780 and HO8910 cells, and the enrichment was more significant in their relative niraparib-resistant cells (Fig. 5K–M), indicating MYC as a key TF involved in the transcriptional regulation of RAD23A in niraparib-resistant ovarian cancer. Next, the effects of SEs on MYC-mediated RAD23A gene transcriptional activation were assessed. The ChIP-qPCR analysis showed that the enrichment of MYC in the RAD23A promoter region was significantly reduced after E1 and E2 knock-out (Fig. 5N), indicating that E1 and E2 knock-out effectively inhibited MYC enrichment in the RAD23A promoter region, thereby affecting its transcriptional activity.

Glycolysis is significantly activated in niraparib-resistant ovarian cancer cells

Glycolysis can drive the malignant progression and drug resistance of tumor cells [23]. Herein, the involvement of glycolysis and histone lactylation were assessed regarding the formation and activation of RAD23A SE during the acquisition of niraparib resistance in ovarian cancer. Therefore, indicators of glycolysis in niraparib-resistant cells, including oxygen consumption rate (OCR), extracellular acidification rate (ECAR), and lactate generation, were assessed. Notably, compared with the non-resistant cells, the OCR in A2780/Nira and HO8910/Nira cells significantly decreased (Fig. 6A), whereas ECAR increased (Fig. 6B); lactate production was significantly increased in the resistant cells (Fig. 6C). Besides, to explore the mechanism of lactate accumulation, we also confirmed that Pyruvate dehydrogenase alpha (PDHA1), the rate limiting enzyme in the pyruvate dehydrogenase complex (PDC), which primes the tricarboxylic acid (TCA) cycle by decarboxylating glycolytically-derived pyruvate to acetyl-CoA [24, 25], remains unchanged in the Niraparib resistant cells compared with parental cells, while the phosphorylation at Ser-232 and Ser-300 of PDHA1 were upregulated (Supplementary Fig. 1A), studies had shown that the phosphorylation of PDHA1 at Ser232 and Ser300 lead to the inactivation of PDHA1 and mediate lactate overproduction [26]. We also detected the levels of monocarboxylate transporters (MCTs), especially MCT1 and MCT4 (MCT1/4) subtypes, which are the main transporters for maintaining lactate homeostasis in tumor cells [27]. Compared with parental cells, the levels of MCT1/4 proteins remained unchanged in niraparib-resistant cells (Supplementary Fig. 1B), and immunofluorescence showed that the localization of MCT1/4 proteins on the cell membrane did not change (Supplementary Fig. 1C). These results indicate that glycolysis is activated in niraparib-resistant ovarian cancer and leads to lactate accumulation. Further in vitro experiments showed that knocking down glycolysis-associated key enzymes pyruvate kinase M (PKM) or lactate dehydrogenase A (LDHA) significantly promoted their sensitivity to niraparib (Fig. 6D), inhibited the proliferation of niraparib-resistant cells (Fig. 6E), and increased the level of DNA damage (Fig. 6F). Conversely, adding exogenous lactate enhanced ovarian cancer cell proliferation and niraparib resistance, and it reduced the level of DNA damage.

Histone lactylation promotes RAD23A expression

Although glycolysis activation in drug-resistant cells leads to lactate accumulation, its effect on RAD23A gene expression is unclear. Therefore, the expression correlation between hexokinase 2, PKM, LDHA, and RAD23A was analyzed in the GEPIA2 and ICGC datasets. Notably, PKM, LDHA, and RAD23A expression were positively correlated (Fig. 7A and B), and the expression of PKM and LDHA was significantly increased in ovarian cancer tissues (Fig. 7C).

To elucidate the regulatory effect of the glycolysis pathway on the transcription and expression of RAD23A via histone lactylation, a pan-lac antibody was used to detect the overall level of lactylation. Notably, the level of lactylation at the histone position in niraparib-resistant cells was significantly increased (Fig. 7D), which was further increased following the addition of exogenous lactate (sodium lactate, Nala) along with RAD23A expression (Fig. 7E-F). Conversely, histone lactylation and RAD23A expression were significantly reduced when ovarian cancer cells were treated with the glycolysis inhibitor 2-deoxy-d-glucose (2-DG) (Fig. 7G). Knock-down of PKM or LDHA in resistant cells markedly decreased mRNA and protein levels of RAD23A, whereas adding exogenous lactate restored RAD23A expression (Fig. 7H and I).

Histone H4K12la promotes RAD23A transcription by activating Nira-SE

To verify the role of histone modification sites in transcriptional regulation, lactylation of four core histones (namely H2A, H2B, H3, and H4) was detected in niraparib-resistant cells. CO-IP results showed that lactylation of H4 was significantly increased in niraparib-resistant cells (Fig. 8A-B). Furthermore, various common lysine residue sites for lactylation were identified in H4, including H4K5la, H4K8la, H4K12la, and H4K16la. Notably, H4K12la exhibited the most significant increase in the resistant cells (Fig. 8C-D). Similarly, exogenous lactate and 2-DG significantly increased and decreased H4K12la levels, respectively (Fig. 8E-F). Additionally, PKM or LDHA knock-down in resistant cells resulted in a decrease in H4K12la levels, while exogenous lactate reversed the effect (Fig. 8G-H). These results indicate that H4K12la lactylation is a key histone modification site regulating niraparib-resistant ovarian cancer cells.

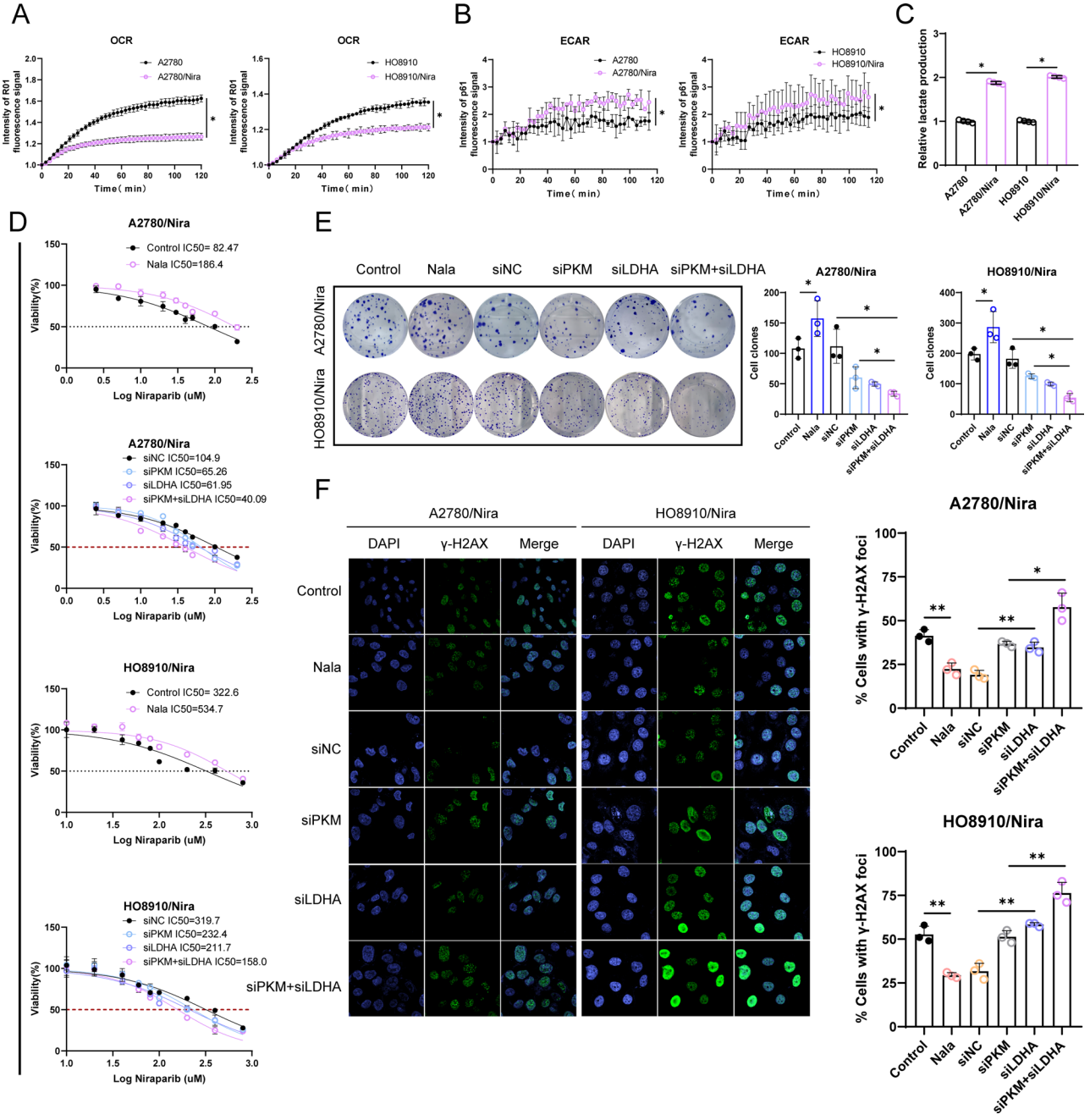

Fig. 6 Glycolysis is significantly activated in niraparib-resistant ovarian cancer cells. (**A**) OCR assay to detect oxygen consumption rate in A2780/Nira, HO8910/Nira and their parental cells. (**B**) ECAR assay to detect extracellular acidification rate in A2780/Nira, HO8910/Nira and their parental cells. (**C**) Detection of changes in lactate content in A2780/Nira, HO8910/Nira and their parental cells. (**D**) Detection of Niraparib IC50 after knockdown of the key enzymes of glycolysis and addition of exogenous lactate in ovarian cancer resistant cells. (**E**) Clone formation assay to detect proliferation ability of ovarian cancer resistant cells after knockdown of the key enzymes of glycolysis and addition of exogenous lactate. (**F**) Immunofluorescence to detect the level of DNA damage marker γ-H2AX after knockdown of the key enzymes of glycolysis and addition of exogenous lactate in ovarian cancer resistant cells. Nala: Sodium L-lactate. ns means $p > 0.05$, $^{*}p < 0.05$, $^{**}p < 0.01$

The transcriptional regulatory mechanism of H4K12la on the target gene RAD23A was further verified by detecting the enrichment of H4K12la in the promoter, E1, and E2 regions of the RAD23A gene. The ChIP assay results showed that H4K12la was enriched in the promoter, E1, and E2 regions of the RAD23A gene in the non-resistant parental cells (Fig. 8I and J). Additionally, the enrichment of H4K12la in the promoter and enhancer regions of the RAD23A gene increased in niraparib-resistant cells (Fig. 8K and L). Besides, the

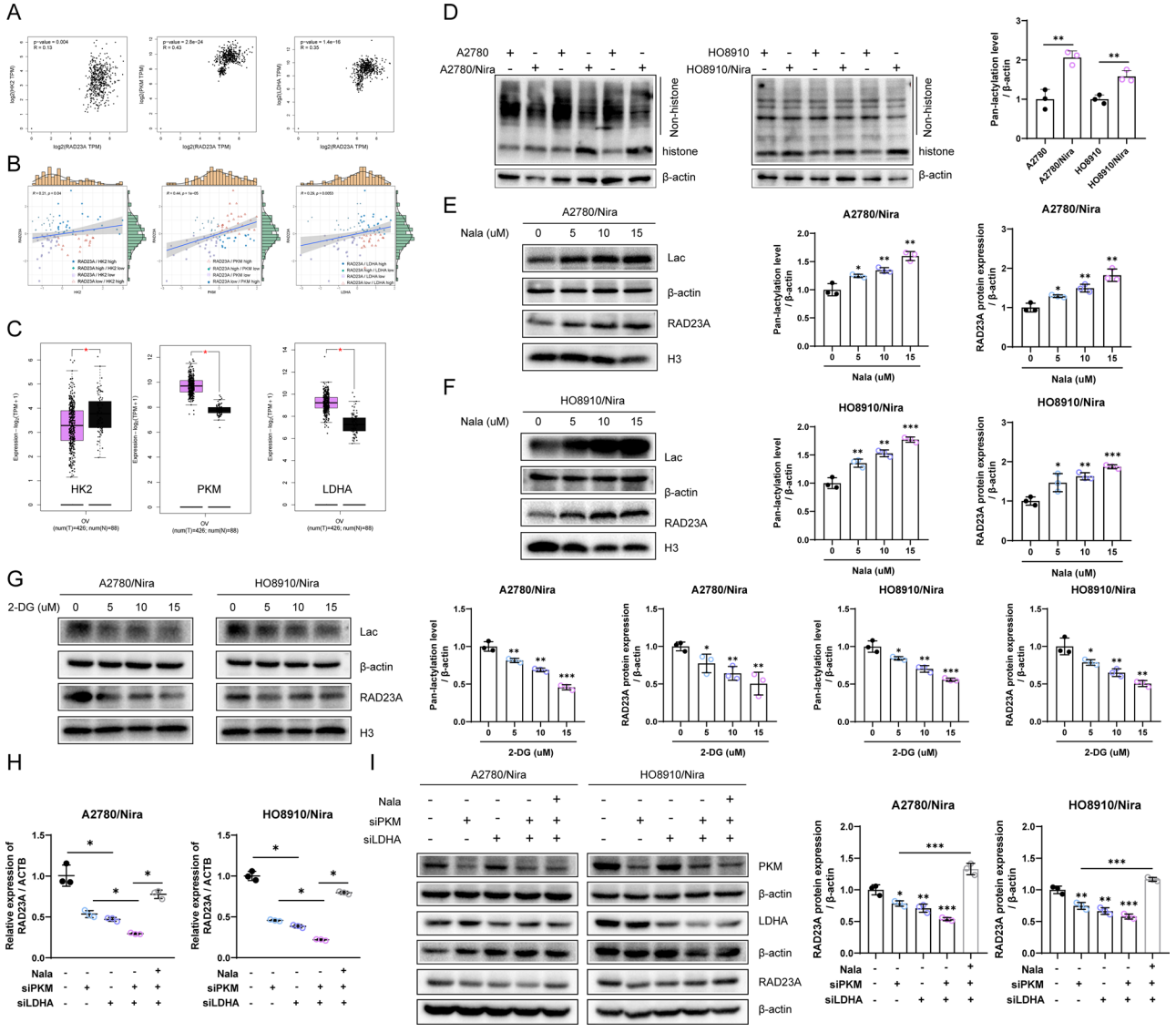

Fig. 7 Histone lactylation promotes RAD23A expression levels. (**A**-**B**) The correlation between key glycolysis enzymes HK2, PKM, LDHA and RAD23A was analyzed in the GEPIA2 and ICGC datasets. (**C**) The expression of HK2, PKM and LDHA in ovarian cancer tissues was analyzed in GEPIA2 datasets. (**D**) The overall level of lactylation in parental and niraparib-resistant cells was detected by pan-lactate antibody. (**E**-**F**) The change of the overall level of lactylation in niraparib-resistant cells after adding exogenous lactate was detected. (**G**) The change of the overall level of lactylation in niraparib-resistant cells after adding glycolysis inhibitor 2-DG was detected. (**H**-**I**) After knocking down PKM or LDHA in ovarian cancer-resistant cells, RAD23A mRNA and protein levels decreased, while the addition of exogenous lactate could restore RAD23A expression. Lac: lactylation, Nala: Sodium L-lactate. ns means $p > 0.05$, $^{*}p < 0.05$, $^{**}p < 0.01$, $^{***}p < 0.001$

knockdown of PKM/LDHA reduced the enrichment of both MYC and H4K12la at promotor/enhancer region of RAD23A (Supplementary Fig. 2); when adding exogenous lactate to A2780 and HO8910 cells, the enrichment of MYC at the RAD23A promoter was increased; while adding glycolysis inhibitor 2-DG to Niraparib resistant cells reduced the enrichment of MYC at the RAD23A promoter (Supplementary Fig. 3). What's more, knocking down of MYC in Niraparib resistant cells didn't influence the enrichment of H4K12la in the promoter, E1, and E2 regions of the RAD23A gene, and there is no direct interaction between H4K12la and Myc (Supplementary Fig. 4). Finally, E1 and E2 knock-out from Nira-SE using CRISPR-Cas9 technology decreased the enrichment of H4K12la in the RAD23A promoter region; this effect could not be reversed by adding exogenous lactate (Fig. 8M). These results indicate that Nira-SE promotes the enrichment of H4K12la lactylation on the target gene promoter, which may be related to its spatial structural function, thereby activating the transcription and expression of RAD23A.

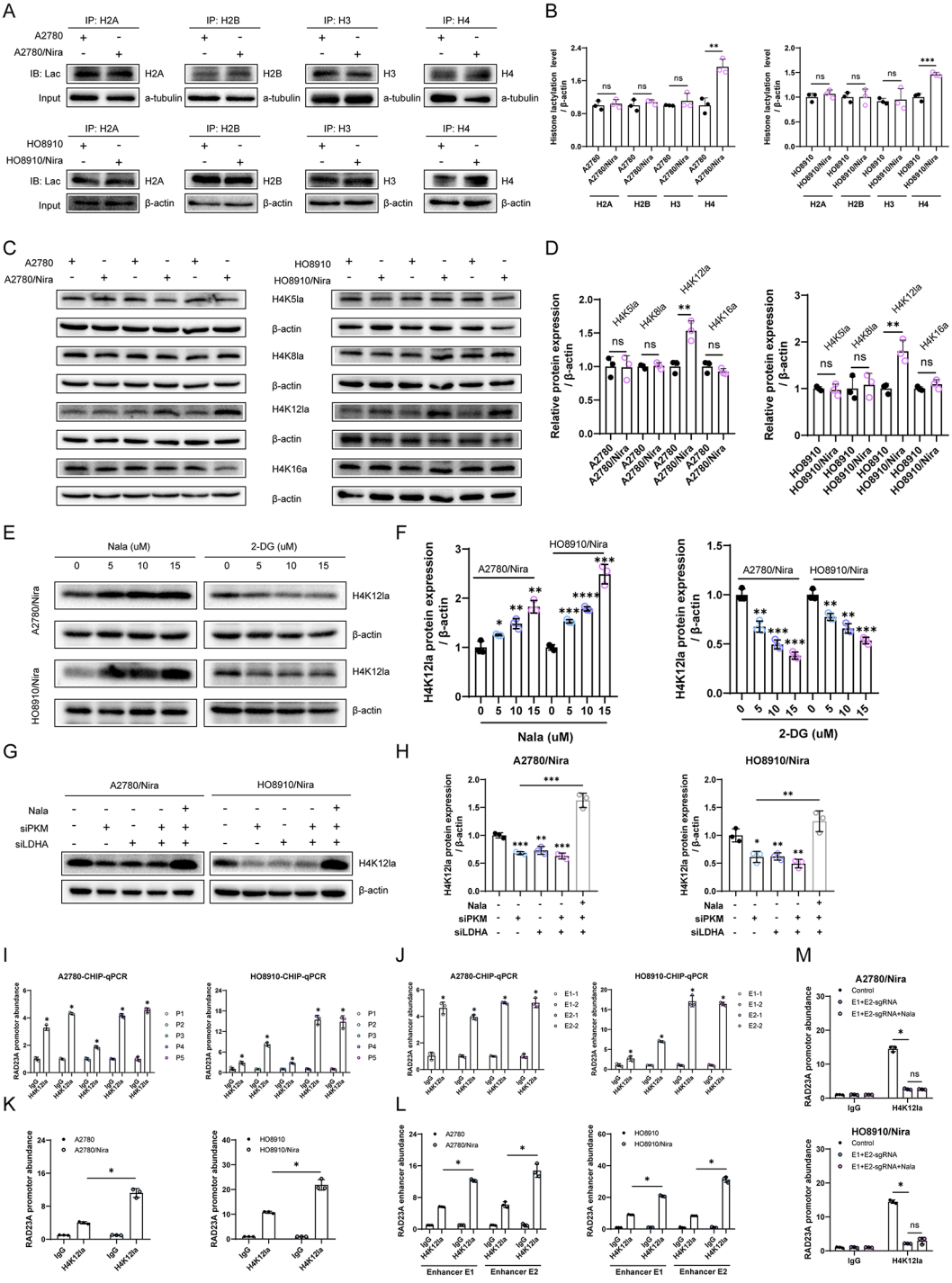

Fig. 8 Histone H4K12la promotes RAD23A transcription by activating the super enhancer Nira-SE. (**A-B**) CO-IP detected the lactylation levels of four core histones (H2A, H2B, H3, H4) in ovarian cancer niraparib-resistant cells, among which the lactylation level of histone H4 was significantly increased. (**C-D**) The lactylation levels of common sites of histone H4 were detected in ovarian cancer resistant cells, among which the lactylation level of H4K12la was significantly increased. (**E-F**) Adding exogenous lactate to ovarian cancer resistant cells can significantly increase the level of H4K12la, while adding the glycolysis inhibitor 2-DG significantly reduces the level of H4K12la. (**G-H**) The changes of H4K12la after knocking down the key glycolysis enzymes PKM and LDHA in ovarian cancer resistant cells and adding exogenous lactate. (**I-J**) The enrichment of H4K12la in the RAD23A promoter and enhancers E1 and E2 was detected in ovarian cancer parental cells. (**K-L**) CHIP-qPCR showed that the enrichment of H4K12la increased on the RAD23A promoter and enhancers E1 and E2 in ovarian cancer resistant cells. (**M**) CHIP-qPCR showed that the enrichment of H4K12la in the RAD23A promoter region decreased after knocking out the core regions E1 and E2 of the super enhancer Nira-SE, and the addition of exogenous lactate could not restore it. Lac: lactylation, Nala: Sodium L-lactate. ns means $p > 0.05$, *$p < 0.05$, **$p < 0.01$, ***$p < 0.001$, ****$p < 0.0001$

Discussion

Drug resistance is a major cause of mortality in many patients with cancer, as drug resistance in tumor cells is often accompanied by metabolic changes, epigenetic reprogramming, and enhanced immune escape ability [28–30]. Herein, a direct association was established between niraparib resistance in ovarian cancer, histone lactylation modification, SEs, and DNA damage repair. In the chemoresistance of ovarian cancer cells to niraparib, the SE located upstream of the RAD23A gene was abnormally activated, which markedly increased the transcriptional activity of RAD23A, which is involved in the early recognition of DNA damage signals in the NER pathway. Simultaneously, active glycolysis was detected in resistant cells, which led to lactate accumulation, and thus, increased lactylation of H4K12la. Notably, H4K12la was enriched in the RAD23A SE and promoter regions, indicating that lactate-mediated histone lactylation acts as an important signal for gene expression regulation. The increase in H4K12la modification in drug-resistant cells resulted in the recruitment of oncogenic TF MYC in the promoter region, thereby activating the RAD23A gene transcription process, enhancing DNA damage repair ability, and promoting drug resistance in ovarian cancer.

Richard A. Young introduced SEs, a type of cis-regulatory element with powerful transcriptional activation functions, in 2013 [6]. Unlike classic enhancers, SEs can comprise multiple enhancers, exhibiting a greater span range than that of a single enhancer. Additionally, SEs are enriched with higher levels of histone modification markers (such as H3K27ac and H3K4me1), bromodomain containing 4, P300/CREB-binding protein, and TFs [31]. Emerging high-throughput sequencing methods such as RIC-seq and Global Run-on Sequencing can detect this activation characteristic of SEs, especially RIC-seq technology, which can indirectly depict the connection between enhancers and promoters. Many studies have reported the association of tissue-specific SEs with cancer development, metastasis, and chemotherapy resistance. For example, SEs in nasopharyngeal carcinoma can promote tumor growth by driving the expression of SOX2 [32]. Additionally, in diffuse large B-cell lymphoma (DLBCL), super-mutated SEs have been reported to prevent the binding of transcription repressors to target genes to downregulate transcription, leading to significant enhancement of proto-oncogenes such as B-cell lymphoma (BCL)6, BCL2, and C-X-C motif chemokine receptor 4, thereby enhancing DLBCL progression [33]. In tamoxifen-resistant estrogen receptor (ER) α-positive breast cancer, ERα can activate related target genes by occupying SE regions, inducing a phosphorylation cascade reaction of the rat sarcoma/rapidly accelerated fibrosarcoma/mitogen-activated protein kinase kinase 2/extracellular signal-regulated kinase/p90RSK/ERα pathway, and promoting the malignant phenotype of ERα-positive breast cancer [34]. Reportedly, Kelly et al. used multi-omics to analyze 86 SEs that were preferentially amplified in patients with ovarian cancer, associating the carcinogenicity of ovarian cancer with activated SEs [10]. Previously, abnormal activation of identified SEs and their target gene RAD23A has been reported in a niraparib-resistant ovarian cancer cell line using the RIC-seq technology.

RAD23A is involved in the early steps of the NER process, mainly recognizing and binding to DNA damage regions. The NER pathway is a highly conserved and multifunctional DNA repair pathway responsible for removing DNA helix damage caused by external factors [35]. Human RAD23 protein forms a DNA repair complex with XPC, co-localizes in the nucleus, and recognizes DNA damage [36]; consequently, defects in the NER pathway can lead to various diseases, including xeroderma pigmentosum, Cockayne syndrome, and trichothiodystrophy. Reportedly, the incidence of skin cancer in patients with NER deficiency is extremely high [37]. In multiple myeloma (MM), NER inhibition has been shown to significantly increase the sensitivity of MM to alkylating agents [38]. Similarly, in vitro, in vivo, and organoid experiment results of this study showed that RAD23A inhibition notably increased the sensitivity of ovarian cancer to niraparib. Moreover, immunofluorescence and comet assay results, evaluating DNA damage levels, showed RAD23A inhibition resulted in decreased DNA damage repair ability in drug-resistant ovarian cancer cells, while RAD23A overexpression could increase DNA damage repair ability in ovarian cancer cells. These results suggested that targeting RAD23A and the associated NER repair pathway may be an effective strategy to overcome niraparib resistance.

The biomolecular and energy requirements of ovarian cancer are primarily met by active glycolysis, a key marker of ovarian cancer [39, 40]. Lactic acid, a product of glycolysis, was previously considered a byproduct of metabolism until Zhang et al. [15]. showed its role as an epigenetic regulator via histone lysine residue lactylation. In recent years, many studies have demonstrated the involvement of histone lactylation in various cell biological processes, such as tumor progression and drug resistance. For example, in promyelocytic leukemia, histone lactylation has been reported to enhance the expression of m1A demethylase AlkB homolog 3, alpha-ketoglutarate dependent dioxygenase, thereby increasing the m1A demethylation of SP100A and promoting tumor progression [41]. Notably, H3K18la lactylation can promote bevacizumab resistance in colorectal cancer by upregulating the expression of autophagy protein rubicon-like autophagy enhancer [42]. In bladder cancer, H3K18la has been reported to promote cisplatin resistance by driving the

expression of key TFs Y box binding protein 1 and YY1 [43]. In general, histone lactylation, as an active enhancer and promoter marker, exhibits a strong gene transcription activation effect. Herein, niraparib-resistant cells exhibited more active glycolysis than non-resistant cells, leading to lactate accumulation. Correlation analysis showed that both PKM and LDHA were significantly positively correlated with RAD23A expression, suggesting the involvement of glycolysis in the transcriptional regulation of RAD23A via histone lactylation. Notably, H4K12la lactylation regulated the activation of Nira-SE and the transcriptional activity of the target gene RAD23A in niraparib-resistant ovarian cancer cells. Nevertheless, the role of histone lactylation in promoting the progression and biological process of ovarian cancer by regulating other important genes and its involvement in the modifications of other histones needs to be further explored.

Conclusion

Overall, the findings of this study showed that the active glycolysis pathway in drug-resistant ovarian cancer leads to increased lactate production and accumulation, further increasing H4K12la lactylation by promoting the recruitment of oncogenic TF MYC in transcriptional regulatory regions to induce the formation of SEs, thereby activating RAD23A expression in the NER pathway. Additionally, the results of xenograft tumor models of ovarian cancer organoids and resistant cells confirmed that targeting RAD23A restored the sensitivity of ovarian cancer to niraparib. In summary, this study elucidated the mechanisms of glycolysis and histone lactylation in regulating gene expression in niraparib resistance in ovarian cancer, suggesting NER pathway-associated RAD23A as a new therapeutic target for addressing niraparib resistance in ovarian cancer.

Abbreviations

PARPi	Poly ADP Ribose Polymerase Inhibitor
BRCA	Breast Cancer Susceptibility Gene
HRD	Homologous Recombination Deficiency
SEs	Super-Enhancers
TFs	Transcription Factors
NER	Nucleotide Excision Repair
RAD23A	RAD23 Homolog A, Nucleotide Excision Repair Protein
OCR	Oxygen Consumption Rate
ECAR	Extracellular Acidification Rate
Nala	Sodium L-Lactate
Lac	Lactylation

Supplementary Information

The online version contains supplementary material available at https://doi.org/10.1186/s12943-025-02295-w.

Supplementary Material 1

Supplementary Material 2

Acknowledgements

Not applicable.

Author contributions

YZ designed the experiments, revised the manuscript and applied for fundings. BFL, YPD and JY performed the cell and molecular biology experiments. BFL wrote the manuscript, analyzed datas and created graphs. JLW and LFZ was responsible for bioinformatics analysis and visualization. XC, XG, QHW and XCH constructed organoid models and performed in vivo experiments. SC collected ovarian tissue and was responsible for project management. All authors read and approved the final manuscript.

Funding

This work was supported by the Project for Key Medicine Discipline Construction of Guangzhou Municipality, CHN [No. 2021-2023-17], Science and Technology Projects in Guangzhou [No. 2024A03J0897], National Natural Science Foundation of China [No. 82203681].

Data availability

No datasets were generated or analysed during the current study.

Declarations

Ethics approval and consent to participate

The Ethics Committee of the third affiliated Hospital of Guangzhou Medical University [NO: 2024 – 301] and Liaoning Cancer Hospital & Institute [NO: KY20231103] approved the use of human tissue in this study. Informed consent was obtained from all patients. Animal experiments were approved by the Experimental Animal Ethics Committee of Guangzhou Medical University [NO: S2024-004].

Consent for publication

All authors have reviewed the final version of the manuscript and approve it for publication.

Competing interests

The authors declare no competing interests.

Author details

[1]Department of Obstetrics and Gynecology, Department of Gynecologic Oncology Research Office, Guangzhou Key Laboratory of Targeted Therapy for Gynecologic Oncology, Guangdong Provincial Key Laboratory of Major Obstetric Diseases, Guangdong Provincial Clinical Research Center for Obstetrics and Gynecology, Guangdong-Hong Kong-Macao Greater Bay Area Higher Education Joint Laboratory of Maternal-Fetal Medicine, The Third Affiliated Hospital, Guangzhou Medical University, No.63 Duobao Raod, Liwan District, Guangzhou, Guangdong Province, P. R. China
[2]Cancer Hospital of China Medical University, Cancer Hospital of Dalian University of Technology, Liaoning Cancer Hospital & Institute, Shenyang, China

Received: 24 September 2024 / Accepted: 5 March 2025
Published online: 19 March 2025

References

1. Siegel RL, Miller KD, Wagle NS, Jemal A. Cancer statistics, 2023. CA Cancer J Clin. 2023;73(1):17–48.
2. Holmes D. Ovarian cancer: beyond resistance. Nature. 2015;527(7579):S217.
3. Christie EL, Bowtell DDL. Acquired chemotherapy resistance in ovarian cancer. Ann Oncol. 2017;28(suppl8):viii13–5.
4. Penn CA, Wong MS, Walsh CS. Cost-effectiveness of maintenance therapy based on molecular classification following treatment of primary epithelial ovarian Cancer in the united States. JAMA Netw Open. 2020;3(12):e2028620.
5. Li GH, Qu Q, Qi TT, Teng XQ, Zhu HH, Wang JJ, et al. Super-enhancers: a new frontier for epigenetic modifiers in cancer chemoresistance. J Exp Clin Cancer Res. 2021;40(1):174.

6. Whyte WA, Orlando DA, Hnisz D, Abraham BJ, Lin CY, Kagey MH, et al. Master transcription factors and mediator Establish super-enhancers at key cell identity genes. Cell. 2013;153(2):307–19.
7. Spitz F, Furlong EE. Transcription factors: from enhancer binding to developmental control. Nat Rev Genet. 2012;13(9):613–26.
8. Sur I, Taipale J. The role of enhancers in cancer. Nat Rev Cancer. 2016;16(8):483–93.
9. Lin X, Spindler TJ, de Souza Fonseca MA, Corona RI, Seo JH, Dezem FS, et al. Super-Enhancer-Associated LncRNA UCA1 interacts directly with AMOT to activate YAP target genes in epithelial ovarian Cancer. iScience. 2019;17:242–55.
10. Kelly MR, Wisniewska K, Regner MJ, Lewis MW, Perreault AA, Davis ES, et al. A multi-omic dissection of super-enhancer driven oncogenic gene expression programs in ovarian cancer. Nat Commun. 2022;13(1):4247.
11. Slyskova J, Sabatella M, Ribeiro-Silva C, Stok C, Theil AF, Vermeulen W, et al. Base and nucleotide excision repair facilitate resolution of platinum drugs-induced transcription blockage. Nucleic Acids Res. 2018;46(18):9537–49.
12. Bowden NA. Nucleotide excision repair: why is it not used to predict response to platinum-based chemotherapy? Cancer Lett. 2014;346(2):163–71.
13. Yokoi M, Hanaoka F. Two mammalian homologs of yeast Rad23, HR23A and HR23B, as multifunctional proteins. Gene. 2017;597:1–9.
14. Hsu PP, Sabatini DM. Cancer cell metabolism: Warburg and beyond. Cell. 2008;134(5):703–7.
15. Zhang D, Tang Z, Huang H, Zhou G, Cui C, Weng Y, et al. Metabolic regulation of gene expression by histone lactylation. Nature. 2019;574(7779):575–80.
16. Nanki Y, Chiyoda T, Hirasawa A, Ookubo A, Itoh M, Ueno M, et al. Patient-derived ovarian cancer organoids capture the genomic profiles of primary tumours applicable for drug sensitivity and resistance testing. Sci Rep. 2020;10(1):12581.
17. Chen X, Liu X, Li QH, Lu BF, Xie BM, Ji YM, et al. A patient-derived organoid-based study identified an ASO targeting SNORD14E for endometrial cancer through reducing aberrant FOXM1 expression and beta-catenin nuclear accumulation. J Exp Clin Cancer Res. 2023;42(1):230.
18. Cai Z, Cao C, Ji L, Ye R, Wang D, Xia C, et al. RIC-seq for global in situ profiling of RNA-RNA Spatial interactions. Nature. 2020;582(7812):432–7.
19. Tang Z, Kang B, Li C, Chen T, Zhang Z. GEPIA2: an enhanced web server for large-scale expression profiling and interactive analysis. Nucleic Acids Res. 2019;47(W1):W556–60.
20. Yeung TL, Leung CS, Wong KK, Samimi G, Thompson MS, Liu J, et al. TGF-beta modulates ovarian cancer invasion by upregulating CAF-derived versican in the tumor microenvironment. Cancer Res. 2013;73(16):5016–28.
21. Gyorffy B. Discovery and ranking of the most robust prognostic biomarkers in serous ovarian cancer. Geroscience. 2023;45(3):1889–98.
22. Andersson R, Gebhard C, Miguel-Escalada I, Hoof I, Bornholdt J, Boyd M, et al. An atlas of active enhancers across human cell types and tissues. Nature. 2014;507(7493):455–61.
23. Icard P, Shulman S, Farhat D, Steyaert JM, Alifano M, Lincet H. How the Warburg effect supports aggressiveness and drug resistance of cancer cells? Drug Resist Updat. 2018;38:1–11.
24. Yang D, Wang Y, Qi T, Zhang X, Shen L, Ma J, et al. Phosphorylation of pyruvate dehydrogenase inversely associates with neuronal activity. Neuron. 2024;112(6):959–71. e8.
25. Stacpoole PW, Dirain CO. The pyruvate dehydrogenase complex at the epigenetic crossroads of acetylation and lactylation. Mol Genet Metab. 2024;143(1–2):108540.
26. Araki R, Hoki Y, Suga T, Obara C, Sunayama M, Imadome K, et al. Genetic aberrations in iPSCs are introduced by a transient G1/S cell cycle checkpoint deficiency. Nat Commun. 2020;11(1):197.
27. Tasdogan A, Faubert B, Ramesh V, Ubellacker JM, Shen B, Solmonson A, et al. Metabolic heterogeneity confers differences in melanoma metastatic potential. Nature. 2020;577(7788):115–20.
28. Goncalves AC, Richiardone E, Jorge J, Polonia B, Xavier CPR, Salaroglio IC, et al. Impact of cancer metabolism on therapy resistance - Clinical implications. Drug Resist Updat. 2021;59:100797.
29. Nussinov R, Tsai CJ, Jang H. Anticancer drug resistance: an update and perspective. Drug Resist Updat. 2021;59:100796.
30. Kim TK, Vandsemb EN, Herbst RS, Chen L. Adaptive immune resistance at the tumour site: mechanisms and therapeutic opportunities. Nat Rev Drug Discov. 2022;21(7):529–40.
31. Hnisz D, Abraham BJ, Lee TI, Lau A, Saint-Andre V, Sigova AA, et al. Super-enhancers in the control of cell identity and disease. Cell. 2013;155(4):934–47.
32. Liu SX, Wang C, Lin RB, Ding WY, Roy G, Wang HB, et al. Super-enhancer driven SOX2 promotes tumor formation by chromatin re-organization in nasopharyngeal carcinoma. EBioMedicine. 2023;98:104870.
33. Bal E, Kumar R, Hadigol M, Holmes AB, Hilton LK, Loh JW, et al. Super-enhancer hypermutation alters oncogene expression in B cell lymphoma. Nature. 2022;607(7920):808–15.
34. Zheng ZZ, Xia L, Hu GS, Liu JY, Hu YH, Chen YJ, et al. Super-enhancer-controlled positive feedback loop BRD4/ERalpha-RET-ERalpha promotes ERalpha-positive breast cancer. Nucleic Acids Res. 2022;50(18):10230–48.
35. Shuck SC, Short EA, Turchi JJ. Eukaryotic nucleotide excision repair: from Understanding mechanisms to influencing biology. Cell Res. 2008;18(1):64–72.
36. van der Spek PJ, Eker A, Rademakers S, Visser C, Sugasawa K, Masutani C, et al. XPC and human homologs of RAD23: intracellular localization and relationship to other nucleotide excision repair complexes. Nucleic Acids Res. 1996;24(13):2551–9.
37. Marteijn JA, Lans H, Vermeulen W, Hoeijmakers JH. Understanding nucleotide excision repair and its roles in cancer and ageing. Nat Rev Mol Cell Biol. 2014;15(7):465–81.
38. Szalat R, Samur MK, Fulciniti M, Lopez M, Nanjappa P, Cleynen A, et al. Nucleotide excision repair is a potential therapeutic target in multiple myeloma. Leukemia. 2018;32(1):111–9.
39. Li C, Liu FY, Shen Y, Tian Y, Han FJ. Research progress on the mechanism of Glycolysis in ovarian cancer. Front Immunol. 2023;14:1284853.
40. Tyagi K, Mandal S, Roy A. Recent advancements in therapeutic targeting of the Warburg effect in refractory ovarian cancer: A promise towards disease remission. Biochim Biophys Acta Rev Cancer. 2021;1876(1):188563.
41. Gu X, Zhuang A, Yu J, Yang L, Ge S, Ruan J, et al. Histone lactylation-boosted ALKBH3 potentiates tumor progression and diminished promyelocytic leukemia protein nuclear condensates by m1A demethylation of SP100A. Nucleic Acids Res. 2024;52(5):2273–89.
42. Li W, Zhou C, Yu L, Hou Z, Liu H, Kong L, et al. Tumor-derived lactate promotes resistance to bevacizumab treatment by facilitating autophagy enhancer protein RUBCNL expression through histone H3 lysine 18 lactylation (H3K18la) in colorectal cancer. Autophagy. 2024;20(1):114–30.
43. Li F, Zhang H, Huang Y, Li D, Zheng Z, Xie K, et al. Single-cell transcriptome analysis reveals the association between histone lactylation and cisplatin resistance in bladder cancer. Drug Resist Updat. 2024;73:101059.

Publisher's note